Identification of Plet-1 as a specific marker of early thymic epithelial progenitor cells

Marianne G. L. Depreter*, Natalie F. Blair*, Terri L. Gaskell*, Craig S. Nowell*, Kathleen Davern†, Adelina Pagliocca*, Frances H. Stenhouse*, Alison M. Farley*, Adrian Fraser*, Jan Vrana*, Kevin Robertson‡, Grant Morahan†, Simon R. Tomlinson*, and C. Clare Blackburn*§

*Medical Research Council/Juvenile Diabetes Research Foundation Centre Development in Stem Cell Biology, Institute for Stem Cell Research and Centre for Regenerative Medicine, University of Edinburgh, King's Buildings, West Mains Road, Edinburgh EH9 3JQ, United Kingdom; ‡Division of Pathway Medicine, University of Edinburgh Medical School, Little France Crescent, Edinburgh EH16 4SB, United Kingdom; and †Western Australian Institute for Medical Research, Perth, Western Australia 6000, Australia

The thymus is essential for a functional immune system, because the thymic stroma uniquely supports T lymphocyte development. We have previously identified the epithelial progenitor population from which the thymus arises and demonstrated its ability to generate an organized functional thymus upon transplantation. These thymic epithelial progenitor cells (TEPC) are defined by surface determinants recognized by the mAbs MTS20 and MTS24, which were also recently shown to identify keratinocyte progenitor cells in the skin. However, the biochemical nature of the MTS20 and MTS24 determinants has remained unknown. Here we show, via expression profiling of fetal mouse TEPC and their differentiated progeny and subsequent analyses, that both MTS20 and MTS24 specifically bind an orphan protein of unknown function, Placenta-expressed transcript (Plet)-1. In the postgastrulation embryo, *Plet-1* expression is highly restricted to the developing pharyngeal endoderm and mesonephros until day 11.5 of embryogenesis, consistent with the MTS20 and MTS24 staining pattern; both MTS20 and MTS24 specifically bind cell lines transfected with *Plet-1*; and antibodies to Plet-1 recapitulate MTS20/24 staining. In adult tissues, we demonstrate expression in a number of sites, including mammary and prostate epithelia and in the pancreas, where Plet-1 is specifically expressed by the major duct epithelium, providing a specific cell surface marker for this putative reservoir of pancreatic progenitor/stem cells. *Plet-1* will thus provide an invaluable tool for genetic analysis of the lineage relationships and molecular mechanisms operating in the development, homeostasis, and injury in several organ/tissue systems.

thymus development | MTS24 | endoderm | mesonephros

The thymus is the central site of T cell generation (1) and therefore is critical for adaptive immunity. The cellularity of the thymus is complex. However, its specialist functions reside largely in the diverse array of thymic epithelial cell (TEC) types that form a key component of the thymic stroma (2–4). Previous work from this and other laboratories has identified and characterized a population of epithelial progenitor cells within the mouse thymic primordium that is sufficient to generate an organized functional thymus containing all TEC subtypes upon ectopic transplantation (5–7). This population is identified by mAbs MTS20 and MTS24 (5, 8). That it contains a common TEPC was initially suggested by the demonstration that the thymus arises solely from the endoderm (9, 10) and was recently confirmed by clonal analysis (11, 12). In the postnatal mouse thymus, MTS20 and MTS24 identify a rare subpopulation of cytokeratin 5⁺ cells located in the thymic medulla and at the corticomedullary junction (6–8), prompting speculation that these may be resident stem/progenitor cells. Consistent with this idea, increased numbers of postnatal MTS24⁺ cells have been reported after induction of thymus regeneration by systemic keratinocyte growth factor (KGF) treatment (13). Recently, MTS24 has also been shown to identify a novel population of putative keratinocyte progenitor/stem cells in the mouse hair follicle (14) that is distinct from the classic follicular stem cell population located in the bulge region (15).

In addition to its utility as a biomarker for TEPC and keratinocyte progenitors, a role for the MTS24 antigen in thymopoiesis has been indicated by function-blocking experiments, in which inclusion of MTS24 completely abrogated T cell development (7). However, despite intensive investigation, the molecular identity of the MTS20 and MTS24 antigens has remained elusive, severely hampering further analysis both of the function of these antigens and of the function, lineage relationships, and requirements of MTS20⁺ and MTS24⁺ cells.

Results

Global Expression Profiling of Mouse TEPC and Their Progeny. To identify markers of TEPC, an *in silico* subtractive strategy was devised based on analysis of global gene expression patterns in TEPC and their presumptive differentiated progeny isolated at day 15.5 of mouse embryonic development (E15.5); a further aim was to identify the genes encoding the MTS20 and MTS24 antigens. Thus, MTS20⁺ TEPC and the corresponding MTS20⁻ epithelial-enriched cell population were obtained from microdissected E15.5 mouse thymic primordia by flow cytometric cell sorting. RNA from 1×10^6 cells pooled from each population was processed for hybridization to Affymetrix MOE430 A and B arrays. The resulting datasets were normalized by using RMA analysis (16) implemented in GENESPRING GX software (Agilent), and assessment of these data using a variety of parameters indicated their high quality. In a pilot analysis designed to investigate the feasibility of identifying TEPC markers using this approach, data from a single E15.5 dataset were filtered using GENESPRING for elements more highly expressed in the MTS20⁺ than the MTS20⁻ populations and were then selected and ranked by fold change to obtain a list obeying the criteria of: 2-fold increase in MTS20⁺ vs. MTS20⁻ datasets and fluorescence intensity >100. This list was further filtered using the GO terms "integral to membrane," "intrinsic to membrane" and "anchored to membrane," and Affymetrix annotation for predicted transmembrane domains (based on the prediction program TMHMM). This analysis was followed by statistical analysis in Limma (http://www.bioconductor.org) (17, 18), after inclusion of two additional E15.5 datasets. *P* values were adjusted by using the Benjamini and Hochberg False Discovery rate (19).

IMMUNOLOGY

Table 1. Relative expression levels of candidates as determined by qRT-PCR

Common name	Relative expression in MTS20+/relative expression in MTS20−	
	E15.5	Postnatal TEC
1600029D21Rik	18 ± 4.5	11,300 ± 1,625*
Cldn4	3.5 ± 0.6	ND
Cldn7	7.8 ± 1.4	ND
Erbb3	1.5 ± 0.4	ND
St14	1.5 ± 0.1	ND
Atp2a3	ND	ND
Fzd3	ND	ND
Atp1b1	1.7 ± 0.1	ND
Ocln	2.1 ± 0.2	ND

The MTS20+CD45−Ter119− and MTS20−CD45-Ter119− populations from E15.5 fetal thymi and epithelial enriched MTS20+CD45−CD11b− fraction from postnatal thymi were isolated and analyzed by real-time PCR with primers specific for the genes listed. Data were normalized by using the geometric mean of three housekeeper genes (*Hprt*, *Hmbs*, and *Ywhaz*) and are presented as fold change of MTS20+ vs. MTS20− cells (±SD) at each time point. Data shown are representative of two technical replicates.
*Postnatal MTS20+ cells were compared to E13.5 MTS20−CD45− TEC.

Genes on the initial list whose subcellular localization was not identified via annotation were then analyzed for the presence of putative transmembrane domains by manual curation. A list of nine candidates remained after these filtering steps: *RIKEN cDNA 1600029D21 gene* (*1600029D21Rik; Plet-1*); *Claudin 4* (*Cldn4*); *Claudin 7* (*Cldn7*); *v-erb-b2 erythroblastic leukemia viral oncogene homolog 3* (*Erbb3*); *suppression of tumorigenicity 14* (*St14*); *ATPase, Ca2+ transporting, ubiquitous* (*Atp2a3*); *frizzled homolog 3* (*Fzd3*); *ATPase, Na+/K+ transporting beta 1 polypeptide* (*Atp1b*); and *occludin* (*Ocln*) [as annotated from the Affymetrix identifiers in NETAFFX, www.affymetrix.com; supporting information (SI) Table 2]. Subsequent qRT-PCR analysis of E15.5 MTS20+ vs. MTS20− epithelium-enriched TECs validated the differential expression of all candidates tested (Table 1). However, a fold change of ≤2 was indicated for four genes, *Ocln, Erbb3, Atp1b1,* and *St14*, and these were excluded from subsequent analysis.

Identification of the MTS20 and MTS24 Antigen. To determine whether the gene(s) encoding the MTS20 or MTS24 antigens were among the remaining candidates, we next analyzed their expression by immunohistochemical and/or qRT-PCR analysis of MTS20+ epithelial cells and MTS20− epithelial-enriched cells obtained from E12.5 thymus primordia and postnatal thymi, focusing initially on the three top-ranked candidates. These analyses excluded Cldn4

and Cldn7 as either the MTS20 or MTS24 antigen, because although these proteins were broadly coexpressed with MTS20 and MTS24 at E12.5–E15.5 (SI Fig. 7) in postnatal thymi, MTS24+ cells formed only a minor subset of Cldn4+ and Cldn7+ cells (Fig. 1). *Plet-1*, however, was highly up-regulated in both E15.5 and postnatal MTS20+ TEPC relative to MTS20−CD45− stromal cells (Table 1), suggesting it as a strong candidate.

Plet-1 was previously identified via an EST screen for placental expressed transcripts, but neither its full developmental expression pattern nor function have been described (20). The expression pattern reported from E5.5 to E8.0 establishes that *Plet-1* is expressed in the ectoplacental cone and extraembryonic ectoderm (E5.5–E8.0) and additionally in the ventral node at E7.5 and E8 (21). Therefore, to determine whether the spatial and temporal expression pattern of *Plet-1* from gastrulation to midgestation in mouse was consistent with that of the MTS20 and MTS24 antigens, *in situ* hybridization (ISH) was carried out on whole embryos from E8.5 to E12.5. During this period, detectable *Plet-1* expression appeared restricted to the pharyngeal endoderm and mesonephros regions (Fig. 2 *A–H*). In addition, weak staining was sometimes apparent in the ectoderm of the pharyngeal clefts. In the pharyngeal endoderm, expression was observed throughout the foregut at E8.5 and was then progressively restricted to the pharyngeal pouches.

These data are highly consistent with those obtained by immunohistochemical staining with MTS20 and MTS24, which E9.5 and E10.5 revealed strong expression throughout the pharyngeal endoderm and pouches (Fig. 2 *I* and *J*), consistent with reported E10.5 staining (7), and in an interlimb stripe that is likely the mesonephros component of the aorta-gonad-mesonephros region in which definitive hematopoietic stem cells arise during fetal development (22). Occasional weaker staining was also seen in the surface ectoderm of the buccal cavity and pharyngeal arches and in mesodermal cells adjacent to the pharyngeal pouches (data not shown).

To further investigate the relationship between *Plet-1* expression and MTS20 and MTS24 staining, qRT-PCR analysis was performed on purified MTS20+ and MTS20− TECs. This revealed dynamic expression of *Plet-1* within the developing thymus primordium; high relative expression levels were observed at E11.5 and thereafter, the level of *Plet-1* decreased markedly until E14.5 (Fig. 3), corresponding to the observed drop in mean fluorescence detected on the surface of most MTS20+ cells by flow cytometry at these time points (6, 7). By E15.5, strong expression was again evident, suggesting either maintenance of high-level expression in a minor population of cells that is purified selectively at E15.5 or reinitiation of high-level expression at this time point (SI Fig. 8). These analyses were again consistent with both flow cytometric and
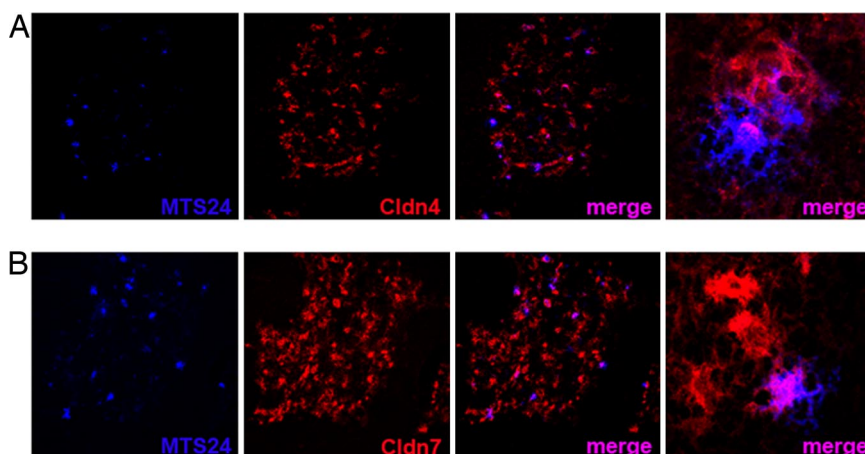
Fig. 1. Expression analysis of candidates excludes Cldn4 and Cldn7. Immunohistochemical analysis showing MTS24 (blue) and (*A*) α-Cldn4 or (*B*) α-Cldn7 (red) staining in the postnatal mouse thymus. Images show sections of postnatal thymus tissue, with Cldn expression restricted to the medulla as previously described (29). The far right in *A* and *B* shows representative high-power images. Most if not all MTS24+ cells express Cldn4 and Cldn7 but are a subset of Cldn4+ and Cldn7+ cells.

Fig. 3. Dynamic regulation of *Plet-1* during thymus organogenesis. Plot shows qRT-PCR analysis of *Plet-1* expression in MTS20⁺CD31⁻CD45⁻Ter119⁻PDGFRα⁻ and MTS20⁻CD31⁻CD45⁻Ter119⁻PDGFRα⁻ cells isolated at different stages of thymus organogenesis. Plet-1 levels are expressed relative to HPRT. Data shown are representative of more than three biological replicates.

Fig. 2. Expression profile of *Plet-1* during mouse embryonic development. (*A–H*) ISH of whole embryos showing specific expression of *Plet-1* in prepouch pharyngeal endoderm at E8.5 (*A* and *B*) and in the pharyngeal pouches and mesonephros from E9.5 to E11.5 (*C–H*). (*I* and *J*) Immunohistochemical staining with MTS24 and α-pancytokeratin (panK) in the pharyngeal region of a representative E9.5 embryo. *B* shows detail from *A* and *D*, detail from *C*. (*H*) shows internal view of hemisected E11.5 embryo. *I* and *J* are serial sections and are representative of the staining seen in at least three separate experiments. en, endoderm; ec, ectoderm; LB, fore limb bud; PP, pharyngeal pouch; pc, pharyngeal cleft; T, tail. Arrows in *A* and *B* indicate pharyngeal endoderm. Arrow in *E* indicates mesonephros region. Arrowheads in *F–H* show third pharyngeal pouch. Arrowhead in *I* indicates oral epithelium in the buccal cavity. Arrowheads in *J* indicate pharyngeal pouches 1–3 (left to right, respectively).

immunohistochemical analyses using MTS20 and MTS24 (SI Fig. 8 and refs. 6 and 7).

The full-length *Plet-1* cDNA was therefore cloned from mouse fetal thymus and transiently expressed in COS-7 cells; the full length *Cldn7* cDNA was also cloned and used as a control in subsequent analyses. *Plet-1*- but not *Cldn7*-transfected COS-7 cells specifically bound both MTS20 and MTS24 at levels consistent with transfection efficiency (shown for MTS20 in SI Fig. 9), suggesting that Plet-1 was the antigen recognized by both MTS20 and MTS24. Stably transfected *Plet-1*-COS-7 cell lines were subsequently generated

and analyzed, confirming this binding specificity (Fig. 4 *A* and *B*). Plet-1 has a predicted molecular mass of 23.2 kDa and, in keeping with this, probing of Western blots of membrane preparations from fetal thymic tissue with MTS20 revealed a band of ≈23 kDa (Fig. 4*C*). Several higher-molecular-mass bands were also observed, consistent with the presence of predicted glycosylation sites in Plet-1 (see below). A rat mAb, 1D4, was subsequently raised to Plet-1 by immunization of rats with the *Plet-1*-COS-7 cells. This mAb revealed a band of the same molecular weight as MTS20 by Western blotting (Fig. 4*C*) and completely colocalized with both MTS20 and MTS24 in the fetal and postnatal thymus by flow cytometric and immunohistochemical analysis (Fig. 4 *D–F*). Collectively, these data establish that Plet-1 is the cognate antigen for both MTS20 and MTS24.

Plet-1 Is an Orphan Protein of Unknown Function. To seek information regarding the likely function of Plet-1, we conducted extensive bioinformatic analyses. Database searches identified *Plet-1* related sequences only in avian and mammalian species (SI Fig. 10) and revealed the existence of two splice variants in the mouse, with alternate exons 4. RT-PCR analysis indicated that "mouse1" is the major and probably only form expressed in the fetal mouse thymus (not shown), and this is also the predominant variant present in the National Center for Biotechnology Information EST database. Further analysis using SignalP and Phobius predicted an amino terminal signal sequence in all *Plet* sequences (SI Fig. 10). Plet-1 is annotated as having a C-terminal transmembrane (TM) region, and this region is predicted for the mouse1, rat, and hamster sequences using TMHMM. In addition, a GPI anchor was predicted by two independent prediction algorithms in mouse1, rat, and hamster, consistent with reports that the hamster orthologue of Plet-1 is GPI anchored (23). Notably, "mouse2" lacks both the GPI anchor and TM sites (SI Fig. 10), suggesting the existence of a secreted isoform. Other than these features and a number of potential glycosylation sites, we found no known functional motifs in the *Plet-1* coding sequence of any species. Although ProSite identified a region of homology with Threonine-rich region/Ig and major histocompatibility complex domain/Type I antifreeze protein containing protein, this was not considered significant because of the high likelihood of this pattern arising by chance.

As described, *Plet-1* is poorly conserved between species (20); only 34% identity exists between mouse Plet-1 and the human orthologue predicted by sequence. Neither MTS20 nor MTS24 bind fetal or postnatal human thymus tissue (data not shown). Although this could be explained by a lack of conserved epitopes, a recent
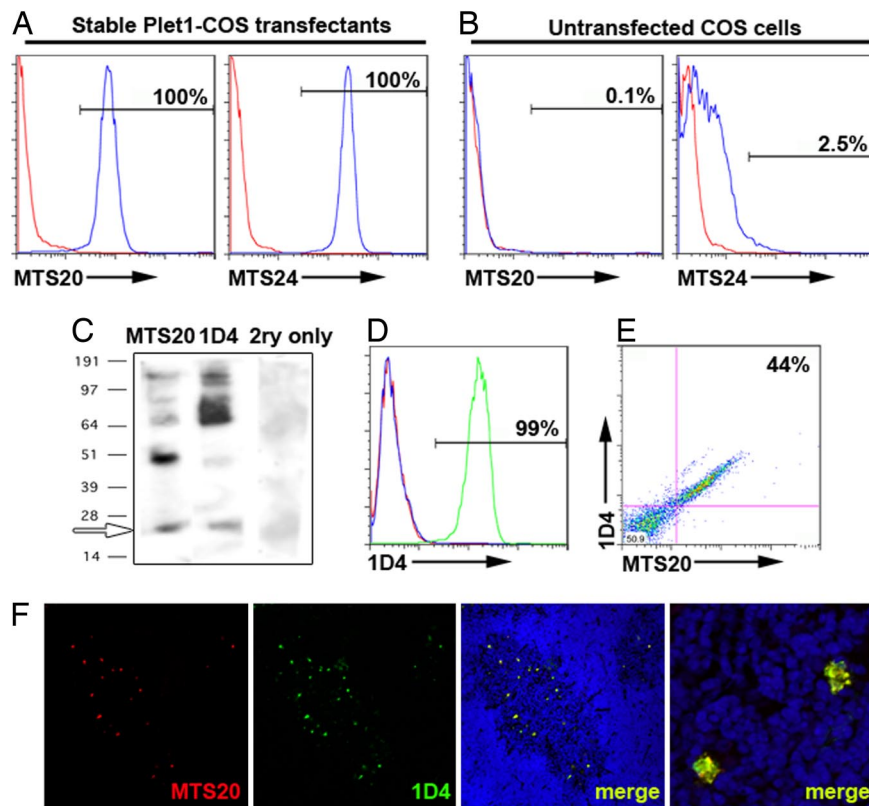
IMMUNOLOGY

Fig. 4. Identification of Plet-1 as the MTS20 and MTS24 antigen. (*A* and *B*) Flow cytometric analysis showing specific binding of MTS20 and MTS24 to COS cells transfected stably with *Plet-1* (*A*) but not to untransfected COS cells (*B*) (blue lines). Isotype controls are shown in red. (*C*) Western blots of membrane fractions obtained from E12.5 thymic tissue were probed with MTS20, 1D4, or appropriate isotype controls. A specific band of ≈23 kDa is revealed by both mAbs (arrow). (*D*) 1D4 binds stable Plet-1-CHO cell transfectants (green line) but does not bind the parental CHO line (red line). Blue line shows isotype control on Plet-1-CHO transfectants. (*E*) Flow cytometric analysis of the E12.5 thymus primordium showing complete colocalization of 1D4 and MTS20. (*F*) Immunohistochemical analysis of postnatal mouse thymus tissue showing complete co-localization of 1D4 (green) and MTS20 (red). Nuclear counterstain is DAPI (blue).

report has indicated suboptimal splice donor and acceptor sites at exons 2 and 3 of human *Plet-1*, rendering expression of its mRNA highly inefficient (20). Consistent with this, analysis of microarray datasets available in the public domain revealed no evidence of human *Plet-1* expression. Therefore, to determine whether *Plet-1* was expressed during human thymus development, day 54 to day 70 human fetal thymus tissue was obtained with full ethical approval and consent, and used to generate cDNA. Thymus development at these stages is equivalent to that at E9.5–E11.5 in the mouse, based on phenotypic and morphological analyses (A.M.F., L. Morris, and C.C.B., unpublished work). Extensive RT-PCR analysis of this cDNA using primers against human *Plet-1* failed to reveal expression of this gene (Fig. 5*A*), although other thymus-specific transcripts including *Foxn1* were readily detected (Fig. 5*A*), and the *huPlet-1*-specific primers amplified the appropriate fragments from human genomic DNA (Fig. 5*B*).
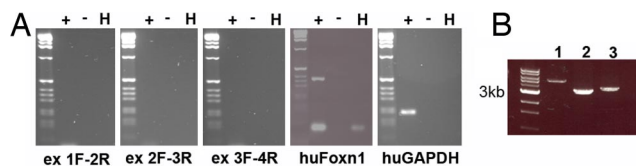
Fig. 5. *Plet-1* is not expressed in human thymus development. (*A*) RT-PCR analysis of day 60 human fetal thymus shows no evidence of *Plet-1* expression. Images show results of amplification with primer pairs predicted to amplify products from exons (ex) 1–2, 2–3, and 3–4 of *Plet-1* and using *Foxn1*- and *GAPDH*- specific primers. The predicted bands were amplified for both *Foxn1* and *GAPDH*. H, no template (water) control; + and −, plus or minus reverse transcriptase. (*B*) PCR analysis of genomic DNA validates the *Plet-1*-specific primers used in *A*. Image shows the predicted bands of 4.9 kb for exon1F and exon2R (lane 1), 2.9 kb for exon2F and exon3R (lane 2), and 3.3 kb for exon3F and exon4R (lane 3), specifically amplified from genomic DNA. Markers (far left lane) are 1-kb ladder.

Plet-1 Is a Marker of Pancreatic Duct Epithelium. It was previously suggested that MTS24 might mark a common endodermal progenitor cell early in mouse development (7). Therefore, we investigated the distribution of this protein in endodermal organ primordia in further detail, focusing on the pancreas because of the importance of identifying cell types that can generate pancreatic beta cells. Consistent with the ISH analysis, no staining was detected at E9.5 or E10.5 in the midgut endoderm caudal to the pharyngeal region. This, together with the expression pattern reported in earlier development (21), indicates that Plet-1 is unlikely to mark a common endodermal progenitor. However, MTS24 staining was detected at E11.5 and from E13.5 to E15.5 in a small group of cells in the epithelial region of the pancreas (SI Fig. 11*A*) and was also observed in the fetal liver (not shown). In adult tissues, MTS24 has been reported to identify a novel population of keratinocyte progenitor/stem cells (14) and is known to bind several other tissues (6, 7). To determine whether it may be a generic marker of epithelial stem/progenitor cells, we surveyed MTS24/Plet-1 expression in selected additional postnatal tissues. MTS24 bound epithelial cells in mammary (Fig. 6*A*, SI Fig. 11*B*) and prostate tissue (not shown), although localization was not restricted to recently described epithelial stem/progenitor pools in either tissue (24–26). In kidney, it colocalized with Cldn4 in medullary collecting ducts (Fig. 6*B*) (27). In the small intestine, MTS24 identified CD45+ cells within Peyer's and Crypto patches but did not bind any cells in the intestinal crypts (Fig. 6*C*). Staining of adult pancreas however revealed MTS24 binding to the epithelium of the major ducts, confirmed by colocalization with the duct-specific markers anti-pan cytokeratin (Fig. 6*D*) and DBA lectin (not shown). MTS24 therefore provides a specific cell surface marker for this cell type, which is strongly implicated as the source of facultative islet stem/progenitor cells induced in some pancreatic injury models (28, 29).

Discussion

The data presented identify Plet-1 as the cognate antigen for mAbs MTS20 and MTS24, which have previously been shown to identify

Fig. 6. Expression of Plet-1 protein in selected postnatal tissues. Immunohistochemical staining of postnatal tissue with MTS24, α-CD49f, α-pancytokeratin (panK), α-Cldn4, as indicated. (*A*) Postnatal mammary gland; MTS24 stains ductal epithelial cells but is not restricted to the CD49f^{bright} fraction that contains stem cells (24). Images show staining in a representative duct. (*B*) Kidney; MTS24 colocalizes with Cldn4 in the medullary collecting ducts (27). *Right* (merge) shows high-power image of sections in *Left* and *Center*. (*C*) Small intestine; MTS24 specifically identifies Peyers and Crypto Patches (arrows). *Left*

and *Center* indicate representative structures; *Right* shows colocalization of MTS24 with CD45 in the small intestine. (*D*) Pancreas; MTS24 stains ductal epithelial cells, as evidenced by colocalization with α-pancytokeratin. Nuclear stain where shown is 7AAD. All images are representative of at least three separate experiments.
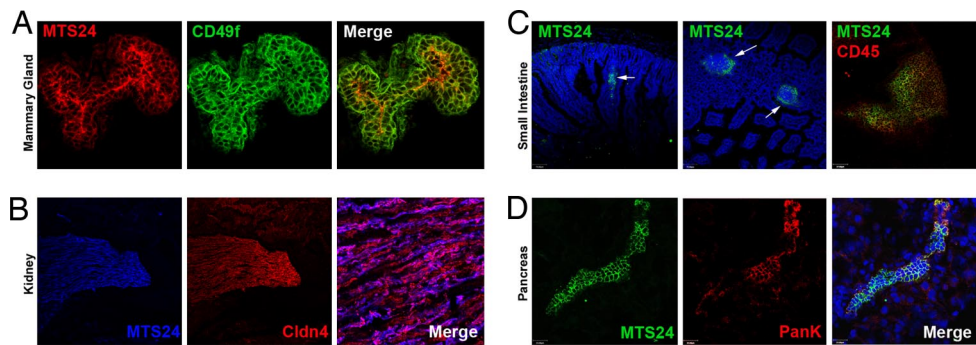
progenitor cell populations in the fetal thymus and postnatal skin in the mouse (6, 7, 14). This finding unifies those of Nijhof *et al.* (14) and Tatefuji *et al.* (23), who independently identified MTS24$^+$ and Plet-1$^+$ populations in mouse and hamster skin. In addition, they indicate MTS24/Plet-1 as a novel marker of pancreatic major duct epithelium, providing the first specific cell surface marker for this putative reservoir of pancreatic stem cells (28, 29), and demonstrate MTS24/Plet-1 expression in mammary and prostate epithelial tissue and in Peyer's and Crypto patches.

This study also identified the tight junction proteins Cldn4 and Cldn7 as candidate markers of TEPC. Expression of Cldn4 has been reported in the fetal and adult mouse thymus (30), whereas Cldn7 has been reported only as a marker of terminally differentiated TECs (31), and our data therefore extend these findings. Although Cldn4 and -7 exhibit a high degree of colocalization with MTS24 at early developmental stages, in the postnatal thymus, MTS24$^+$ cells are a minor subset of Cldn4$^+$ and Cldn7$^+$ cells, suggesting a possible precursor:progeny relationship between the MTS24$^+$ cells and the broader population(s) defined by Claudin expression. These lineage relationships are of particular interest, because Cldn3 and −4, in conjunction with *Ulex europaeus* lectin (UEA-1), have recently been shown to mark precursors for the subset of medullary TEC that express *Autoimmune regulator* (*AIRE1*) (30), a gene that is critically required for induction of self tolerance in the maturing T cell pool.

Collectively, the reported findings will facilitate prospective isolation and functional testing of several medically important cell populations. Furthermore, they enable genetic analysis of the function, lineage potential, and molecular requirements of populations defined on the basis of MTS20 or MTS24 binding during organ/tissue development, homeostasis, and regeneration. We envisage that this advance will contribute important information to understanding of thymus, skin, and pancreas biology and of the fetal hematopoietic stem cell niche, in particular, by permitting definitive evaluation of the role of MTS24$^+$ cells in the fetal and postnatal thymus, and of the capacity of pancreatic ductal epithelium to regenerate β cell mass.

Materials and Methods

Mice. CBAxC57BL/6 F$_1$ mice were used for all analyses. For timed matings, C57BL/6 females were mated with CBA males, and noon of the day of the vaginal plug was taken as E0.5.

Embryo Dissection. Embryos were dissected from the uterus in either PBS or M2 medium (Sigma), then processed for ISH or placed in TRIzol (Invitrogen) for RNA extraction.

Human Fetal Tissue. Human fetal tissue was obtained with full ethical approval and consent from the Centre for Reproductive Biology, University of Edinburgh.

Antibodies. The following mAbs were used for immunofluorescence and flow cytometry: MTS20 (IgM) (8) and MTS24 (IgG$_{2a}$) (5) are rat mAbs that recognize plasma membrane determinants and were a kind gift from R. L. Boyd (Monash University Medical School, Melbourne, Australia); anti-cytokeratin (rabbit polyclonal anti-keratin, Dako); α-CD45 (30-F11; FITC-conjugated); α-CD11b (M1/70; FITC-conjugated); α-CD31 (MEC13.3, R-PE conjugated); α-PDGFRα (APA5); and Ter119 (all BD PharMingen). 1D4 is a rat IgG raised against Plet-1, as described herein. α-Cldn4 and α-Cldn7 (Zymed) are polyclonal sera that recognize intracellular determinants; α-Cldn4 was a kind gift from M. Furuse and S. Tsukita (Kyoto University, Kyoto, Japan). Appropriate isotype-control antibodies (BD PharMingen) provided negative controls in all experiments. Unconjugated mAbs were detected by using mouse anti-rat IgM-PE (BD PharMingen), donkey anti-mouse IgG F(ab')$_2$-FITC, goat anti-rat IgM-Cy3, donkey anti-rat IgG-Cy3, goat anti-rat IgG/M-FITC, and goat anti-rabbit IgG-FITC (all Jackson Laboratories), or goat anti-rabbit IgG-Alexa647 (Invitrogen). TO-PRO3 (Molecular Probes) or DAPI was used as a nuclear counterstain.

Flow Cytometry. Cells were dissociated to single cell suspensions and stained as described (6). Cells were analyzed on a FACSCalibur (Becton Dickinson) and by using FlowJo Ver. 4.4.4 (Tree Star). TO-PRO3 (Molecular Probes) or 7AAD was used to identify dead cells.

Purification of Fetal and Postnatal MTS20$^+$ Cells. Mouse fetal thymi were microdissected, dissociated, and processed for flow cytometry as described (6). MTS20$^+$CD45$^-$Ter119$^-$ and MTS20$^-$CD45$^-$Ter119$^-$ or MTS20$^+$CD31$^-$CD45$^-$Ter119$^-$PDGFRα$^-$ and MTS20$^-$CD31$^-$CD45$^-$Ter119$^-$PDGFRα$^-$ populations were isolated from fetal thymi by flow cytometric sorting, to a purity of >95% for each sample. To isolate postnatal MTS20$^+$ and MTS20$^-$ TEC, thymi were dissected from 2-mo-old mice and digested by using 0.125% (wt/vol) collagenase D at 37°C for 15 min (6). An initial enrichment for epithelial cells was achieved by using a Percoll gradient. Cells collected from the gradient were immunostained by using MTS20 (PE) and the MTS20$^+$ and MTS20$^-$ fractions within the epithelial gate isolated by flow cytometric cell sorting. These fractions were then stained with α-CD45 and α-CD11b (FITC-conjugated) and the MTS20$^+$CD45$^-$CD11b$^-$ and MTS20$^-$CD45$^-$CD11b$^-$ fractions purified by a second sort, routinely to >95% purity; cytospin analysis of sorted cells indicated that >95% of MTS20$^+$ cells were epithelial, based on anti-pancytokeratin staining. Flow cytometric sorting was performed by using a MoFlo (DakoCytomation).

RNA Collection. Intact total RNA was extracted from individual samples by using TRIZOL reagent (Invitrogen) or Qiazol reagent (Qiagen), according to the manufacturer's instructions, and the quality of the RNA determined by analysis on an Agilent Bioanalyser (Agilent Technologies). For global expression profiling, RNA samples were then pooled such that each pool contained RNA from ≈1 × 10^6 cells, DNase treated (DNA-*free*, Ambion), precipitated to the required concentration, and processed for Affymetrix analysis. For qRT-PCR analysis, samples were used individually or pooled as required.

Affymetrix Microarray Analysis. Samples were labeled and hybridized to MOE-430A and -B GeneChip arrays according to standard Affymetrix protocols. The candidate list was obtained by analysis of arrays hybridized with cRNA from E15.5 MTS20$^+$CD45$^-$Ter119$^-$ TEPC and MTS20$^-$CD45$^-$Ter119$^-$ epithelium-enriched stromal cells. Data were analyzed by using GENESPRING GX (Agilent) and Limma (Bioconductor) software.

RT-PCR and Real-Time RT-PCR (qRT-PCR). Total RNA was isolated from microdissected fetal thymus tissue or sorted cell populations as described, and single stranded cDNA was synthesized by using SuperScript II reverse-transcriptase

(Invitrogen) and random hexamers or oligo(dT) primers according to the manufacturer's instructions. RT-PCR was performed by using the primer pairs shown in SI Table 3. For qRT-PCR analysis, gene-specific amplification was performed by using (*i*) the iCycler iQ real-time PCR Detection system (Bio-Rad), using IQ SYBR green Supermix (Bio-Rad) for quantification (Table 1): reactions were run for 40 cycles of 15 sec at 95°C and 60 sec at 60°C, after an initial 8.5 min at 95°C. A dissociation thermal protocol was used to analyze the melting peaks of the products. Relative expression level of the target gene was normalized to the geometric mean of three internal control genes (*Hprt*, *Ywhaz*, and *Hmbs*). Duplicate samples on each plate and technical duplicates were run for each sample. No RT and no template controls were included in all experiments; or (*ii*) a LightCycler 480 (Roche) using the Roche Universal probe library and the Light-Cycler 480 Probes Master (Roche) mastermix (Fig. 3). Specific amplification of *Plet-1* and *HPRT* was detected by using probes 20 and 95, respectively. Primer sequences are shown in SI Table 4.

Cloning. For cloning of mouse *Plet-1* and mouse *Cldn7*, RT-PCR was carried out on cDNA generated from E13.5 mouse thymus RNA, with primers specific for full length mouse *Plet-1* or *Cldn7*. PCR products were subcloned by using the T/A TOPO PCR cloning kit (Invitrogen), sequenced by using BigDye Terminator reaction mix (ABI), and sequences analyzed by using DNAStar software (Ver. 6). The following primers were used: *Plet-1*F GTCGACATGCTGTCGCTCCGGCTCC; *Plet-1*R GCGGCCGCTTAGAAGAGGAGTTTACT; *Cldn7*F GTCGACATGGCCAACTCGGGC-CTG; and *Cldn7*R GCGGCCGCTCACACGTATTCCTTGGA.

Cell Line Generation. The full length sequences encoding *Cldn7* or *Plet-1* were subcloned into pPyCAGIP (32) and transfected into COS-7 or CHO cells by using the standard Lipofectamine 2000 (Invitrogen) protocol; vehicle-only controls were provided by parallel transfection with the eGFP expression plasmid, pPy-CAGGFPIP (32), which was used to estimate transfection efficiency. Transient expression of the respective genes was tested after 60 h by immunostaining and flow cytometry. To generate stably transfected lines expressing GFP, Cldn7 or Plet-1, the cells were placed in selective medium (GMEM containing 2 μg/ml Puromycin) 24–72 h after transfection, and medium was then renewed every 24–48 h. Ten days after transfection, Puromycin-resistant colonies were picked and expanded in selective medium, and expression of the relevant protein confirmed by flow cytometric analysis.

Immunohistochemistry. Eight-micrometer sections were cut and either stained with hematoxylin/eosin or processed for immunohistochemistry, as described (9).

Isotype controls (not shown) were included in all experiments. Staining was analyzed by using a Leica AOBS confocal microscope (Leica). The images presented are either single optical sections or projected focus stacks of serial optical sections.

Western Blotting. Membrane preparations were obtained from E12.5 mouse fetal thymic primordia, as described (7). Proteins were separated by electrophoresis on a SDS/PAGE gel and blotted onto a PVDF membrane according to standard protocols.

ISH. Whole-mount ISH were performed as described (33) by using probes directed to full length or the 3′ UTR of Plet-1 ("mouse" in SI Fig. 10). BM-purple (Roche/BMB) was used to localize the hybridized probe.

Generation of mAbs. Wistar rats were immunized with 1×10^7 COS-7 cells stably transfected with *Plet-1*. Rats received intraperitoneal injections of cells emulsified in Complete Freund's Adjuvant (Difco), followed by a boost in Incomplete Freund's adjuvant 22 days later. Rats were bled 13 days postboost and sera assayed by immunofluorescence (IFA). The best responder was boosted with 1×10^7 cells in PBS 4 days before fusion. Spleen cells were fused with Sp2/O myeloma cells according to standard procedures (34). Antibody-containing supernatants were screened by IFA on transfected and nontransfected cells. Hybridomas producing antibodies which reacted specifically with transfected cells were selected for further study.

Note added in proof. We have recently become aware that the Plet-1 expression pattern from E7.5 to E10.5 has been reported, using GenBank accession no. NM_029639 rather than 1600029D21Rik (35). The findings reported are consistent with those herein, although our interpretation of the Plet-1 E7.5 expression pattern differs from that of Moore-Scott *et al.* (35).

1. Miller JFAP (1961) Immunological function of the thymus. *Lancet* 2:748–749.
2. Anderson G, Jenkinson E (2001) Lymphostromal interactions in thymus development and function. *Nat Rev Immunol* 1:31–40.
3. Blackburn CC, *et al.* (2002) One for all and all for one: thymic epithelial stem cells and regeneration. *Trends Immunol* 23:391–395.
4. Kyewski B, Klein L (2006) A central role for central tolerance. *Annu Rev Immunol* 24:571–606.
5. Blackburn CC, *et al.* (1996) The nu gene acts cell-autonomously and is required for differentiation of thymic epithelial progenitors. *Proc Natl Acad Sci USA* 93:5742–5746.
6. Bennett AR, *et al.* (2002) Identification and characterization of thymic epithelial progenitor cells. *Immunity* 16:803–814.
7. Gill J, Malin M, Hollander GA, Boyd R (2002) Generation of a complete thymic microenvironment by MTS24(+) thymic epithelial cells. *Nat Immunol* 3:635–642.
8. Godfrey DI, Izon DJ, Tucek CL, Wilson TJ, Boyd RL (1990) The phenotypic heterogeneity of mouse thymic stromal cells. *Immunology* 70:66–74.
9. Gordon J, *et al.* (2004) Functional evidence for a single endodermal origin for the thymic epithelium. *Nat Immunol* 5:546–553.
10. Blackburn CC, Manley NR (2004) Developing a new paradigm for thymus organogenesis. *Nat Rev Immunol* 4:278–289.
11. Bleul CC, *et al.* (2006) Formation of a functional thymus initiated by a postnatal epithelial progenitor cell. *Nature* 441:992–996.
12. Rossi SW, Jenkinson WE, Anderson G, Jenkinson EJ (2006) Clonal analysis reveals a common progenitor for thymic cortical and medullary epithelium. *Nature* 441:988–991.
13. Rossi SW, *et al.* (2007) Keratinocyte growth factor (KGF) enhances postnatal T-cell development via enhancements in proliferation and function of thymic epithelial cells. *Blood* 109:3803–3811.
14. Nijhof JG, *et al.* (2006) The cell-surface marker MTS24 identifies a novel population of follicular keratinocytes with characteristics of progenitor cells. *Development* 133:3027–3037.
15. Rochat A, Kobayashi K, Barrandon Y (1994) Location of stem cells of human hair follicles by clonal analysis. *Cell* 76:1063–1073.
16. Irizarry RA, *et al.* (2003) Summaries of Affymetrix GeneChip probe level data. *Nucleic Acids Res* 31:e15.
17. Smyth GK (2004) Linear models and empirical bayes methods for assessing differential expression in microarray experiments. *Stat Appl Genet Mol Biol* 3, Article 3.
18. Smyth GK (2005) in *Bioinformatics and Computational Biology Solutions Using R, Bioconductor*, Gentleman R, Carey V, Dudoit S, Irizarry R, Huber W, eds (Springer, New York), pp 397–420.
19. Benjamini Y, Hochberg Y (1995) Controlling the false discovery rate: a practical and powerful approach to multiple testing. *J Royal Stat Soc B* 57:289–300.
20. Zhao SH, *et al.* (2004) PLET1 (C11orf34), a highly expressed and processed novel gene in pig and mouse placenta, is transcribed but poorly spliced in human. *Genomics* 84:114–125.
21. Frankenberg S, Smith L, Greenfield A, Zernicka-Goetz M (2007) Novel gene expression patterns along the proximo-distal axis of the mouse embryo before gastrulation. *BMC Dev Biol* 7:8.
22. Medvinsky A, Dzierzak E (1996) Definitive hematopoiesis is autonomously initiated by the AGM region. *Cell* 86:897–906.
23. Tatefuji T, *et al.* (2004) Identification of the novel membrane-associated protein AgK114 on hamster keratinocytes recognized by a monoclonal antibody. K114. *Biol Pharm Bull* 27:1742–1749.
24. Stingl J, *et al.* (2006) Purification and unique properties of mammary epithelial stem cells. *Nature* 439:993–997.
25. Shackleton M, *et al.* (2006) Generation of a functional mammary gland from a single stem cell. *Nature* 439:84–88.
26. Taylor RA, *et al.* (2006) Formation of human prostate tissue from embryonic stem cells. *Nat Methods* 3:179–181.
27. Facchetti F, *et al.* (2007) Claudin 4 identifies a wide spectrum of epithelial neoplasms and represents a very useful marker for carcinoma versus mesothelioma diagnosis in pleural and peritoneal biopsies and effusions. *Virchows Arch* 451:669–680.
28. Grapin-Botton A (2005) Ductal cells of the pancreas. *Int J Biochem Cell Biol* 37:504–510.
29. Xu X, *et al.* (2008) Beta cell progenitors can be generated from endogenous progenitors in injured adult mouse pancreas. *Cell*, in press.
30. Hamazaki Y, *et al.* (2007) Medullary thymic epithelial cells expressing Aire represent a unique lineage derived from cells expressing claudin. *Nat Immunol* 8:304–311.
31. Senoo M, Pinto F, Crum CP, McKeon F (2007) p63 is essential for the proliferative potential of stem cells in stratified epithelia. *Cell* 129:523–536.
32. Chambers I, *et al.* (2003) Functional expression cloning of Nanog, a pluripotency sustaining factor in embryonic stem cells. *Cell* 113:643–655.
33. Gordon J, Bennett AR, Blackburn CC, Manley NR (2001) Gcm2 and Foxn1 mark early parathyroid- and thymus-specific domains in the developing third pharyngeal pouch. *Mech Dev* 103:141–143.
34. Goding J (1996) *Monoclonal Antibodies: Principles and Practice* (Academic, London).
35. Moore-Scott BA, Opoka R, Lin SJ, Kordich JJ, Wells JM (2007) Identification of molecular markers that are expressed in discrete anterior–posterior domains of the endoderm from the gastrula stage to midgestation. *Dev Dyn* 236:1997–2003.